

# CUSP SHAPES OF HILBERT-BLUMENTHAL SURFACES

**Joseph Quinn**

JOSEPHANTHONYQUINN@GMAIL.COM  
 NATIONAL MUSEUM OF MATHEMATICS  
 134 W 26TH STREET, SUITE 4-S  
 NEW YORK, NY 10001  
 USA

**Alberto Verjovsky**

ALBERTO@MATCUER.UNAM.MX  
 INSTITUTO DE MATEMÁTICAS, UNIDAD CUERNAVACA  
 UNIVERSIDAD NACIONAL AUTÓNOMA DE MÉXICO  
 AV UNIVERSIDAD S/N, COL. LOMAS CHAMILPA  
 CP 62210, CUERNAVACA, MORELOS  
 MÉXICO

**ABSTRACT.** We introduce a new fundamental domain  $\mathcal{R}_n$  for a cusp stabilizer of a Hilbert modular group  $\Gamma$  over a real quadratic field  $K = \mathbb{Q}(\sqrt{n})$ . This is constructed as the union of Dirichlet domains for the maximal unipotent group, over the leaves in a foliation of  $\mathcal{H}^2 \times \mathcal{H}^2$ . The region  $\mathcal{R}_n$  is the product of  $\mathbb{R}^+$  with a 3-dimensional tower  $\mathcal{T}_n$  formed by deformations of lattices in the ring of integers  $\mathbb{Z}_K$ , and makes explicit the cusp cross section's Sol 3-manifold structure and Anosov diffeomorphism. We include computer generated images and data illustrating various examples.

## 1. INTRODUCTION

A Hilbert-Blumenthal group is some  $\Gamma = \mathrm{PSL}_2(\mathbb{Z}_K)$  where  $\mathbb{Z}_K$  is the ring of integers of a real quadratic field  $K$ , and a Hilbert-Blumenthal surface is a quotient  $M_\Gamma = (\mathcal{H}^2 \times \mathcal{H}^2)/\Gamma$  of the product of two hyperbolic upper half-planes  $\mathcal{H}^2$  by the Möbius action of  $\Gamma$  under Galois conjugation. As a generalization of modular curves,  $M_\Gamma$  represents the moduli space of Abelian varieties with real multiplication by  $\mathbb{Z}_K$  [16] and these complex surfaces are a prototype for Shimura varieties, placing them at an interesting juncture of geometry, topology and number theory.

Here we are motivated by the search for a fundamental domain for the action of  $\Gamma$  on  $\mathcal{H}^2 \times \mathcal{H}^2$  which accurately reflects the geometry of  $M_\Gamma$ , a topic that dates back to Blumenthal [3, 4]. Historically, our understanding of such a domain has improved with our understanding of its cusps. Maass [15] showed that the number of cusps equals the class number of  $K$ ,

---

*Date:* June 28, 2019.

then Siegel [19] computed a fundamental domain as a union over one piece at each cusp using an alternative metric. This yields a complex surface with quotient singularities and cusp singularities, which Hirzebruch [13] showed how to smoothly compactify (see also [20] and §21 of [2]). While these advances have been fruitful in understanding arithmetic and topological properties, certain geometric properties had remained elusive. A cusp (cross) section of  $M_\Gamma$  is a 3-dimensional mapping torus of some Anosov diffeomorphism  $\varphi$  of the torus and, due to McReynolds [17, 18], every Sol 3-manifold is commensurable to one of these cusp sections up to diffeomorphism. However, there had previously been no combinatorial description of these in terms of their sides and the action of  $\varphi$  as an explicit side-pairing map. Here we provide this, subsequently also modeling an example from every commensurability class of the Sol 3-manifolds.

To do this, we weaken the product metric on  $\mathcal{H}^2 \times \mathcal{H}^2$  to a semimetric  $\delta$ , which restricts to a scaled Euclidean metric on each leaf of a natural foliation of the space. This allows us to build a fundamental domain  $\mathcal{B}_n$  for the maximal unipotent subgroup of the cusp stabilizer as a union of toroidal Dirichlet domains in the leaves with respect to  $\delta$ . This region is a 3-dimensional hypersurface  $\mathcal{T}_n$  (modeling the cusp section  $T_\varphi^3$ ) crossed with  $\mathbb{R}^+$ , up to uniformly scaling the metric. The shape of  $\mathcal{T}_n$  is described by lattices from the ring of integers  $\mathbb{Z}_K$  of  $K$  that deform along a common axis of symmetry, in a way that is effectively computable from the fundamental unit  $\varepsilon$  of  $\mathbb{Z}_K$ . The Anosov diffeomorphism is then the diagonal matrix with diagonal  $(\varepsilon, \varepsilon^{-1})$ , which glues one lattice slice to another. We also provide a map  $\Psi_n : \mathcal{H}^2 \times \mathcal{H}^2 \rightarrow \mathbb{R}^3$  with which one can plot the image of  $\mathcal{T}_n$  to visualize the cusp section (see Figure 4).

## 2. PRELIMINARIES

**2.1. Hilbert-Blumenthal surfaces and cusp sections.** Let  $\mathcal{H}^2$  be the upper half-plane model for the hyperbolic plane and denote the usual metric by  $d_{\mathcal{H}^2}$ . We will be interested in the product space  $\mathcal{H}^2 \times \mathcal{H}^2$ , in which the points are of the form  $(x_1 + y_1i, x_2 + y_2i)$  where  $x_1, x_2 \in \mathbb{R}$  and  $y_1, y_2 \in \mathbb{R}^+$ , and we fix this notation throughout. For  $\gamma = \begin{pmatrix} a & b \\ c & d \end{pmatrix} \in \mathrm{PSL}_2(\mathbb{R})$  and  $p \in \mathcal{H}^2$ , let  $\gamma(p)$  denote the usual isometric action by Möbius transformations,

$$\gamma(p) = \frac{ap + b}{cp + d}.$$

Let  $K$  be a real quadratic number field and let  $\sigma$  be the non-trivial element of the Galois group  $\mathfrak{G}(K : \mathbb{Q})$ . That is,  $K = \mathbb{Q}(\sqrt{n})$  for some square-free  $n \in \mathbb{N}$  and  $\forall a, b \in \mathbb{Q}$ , we have  $\sigma(a + b\sqrt{n}) = (a - b\sqrt{n})$ . Let  $\mathbb{Z}_K$  be the ring of integers of  $K$ , i.e.  $\mathbb{Z}_K = \mathbb{Z} \oplus \mathbb{Z}\alpha$  where

$$\alpha := \begin{cases} \sqrt{n} & ; \quad n \not\equiv_4 1 \\ \frac{1+\sqrt{n}}{2} & ; \quad n \equiv_4 1 \end{cases}.$$

Let  $\Gamma := \mathrm{PSL}_2(\mathbb{Z}_K)$  and for  $\gamma \in \Gamma$  let then  $\sigma(\gamma)$  denote the application of  $\sigma$  to the entries of  $\gamma$ . Then

$$\Gamma \curvearrowright \mathcal{H}^2 \times \mathcal{H}^2 : \quad \gamma(p_1, p_2) = (\gamma(p_1), \sigma(\gamma)(p_2))$$

is a discrete action by isometries.

**Definition 2.1.**

- (1) We call  $\Gamma$  a Hilbert-Blumenthal group, and we call the orbifold  $(\mathcal{H}^2 \times \mathcal{H}^2)/\Gamma$  a Hilbert-Blumenthal surface, which we denote by  $M_\Gamma$ .
- (2) For  $p \in \partial(\mathcal{H}^2 \times \mathcal{H}^2)$ , the stabilizer of  $p$  in  $\Gamma$ , is  $\Delta_\Gamma(p) := \{\gamma \in \Gamma \mid \gamma(p) = p\}$ .
- (3) The maximal unipotent subgroup (of  $\Gamma$  at  $p$ ), denoted by  $U_\Gamma(p)$ , is the group of all unipotent elements of  $\Delta_\Gamma(p)$ .
- (4) When  $U_\Gamma(p) \neq \emptyset$ , we say that that  $\Gamma$  (or equivalently that  $(\mathcal{H}^2 \times \mathcal{H}^2)/\Gamma$ ) has a cusp at  $p$ , and in this case we call  $\Delta_\Gamma(p)$  a cusp group.

**Remark 2.2.** For  $\gamma \in \Delta_\Gamma(p)$ , the condition that  $\gamma \in U_\Gamma(p)$  is equivalent to saying that  $\gamma$  has a unique fixed point as an isometry of  $\mathcal{H}^2 \cup \partial\mathcal{H}^2$ , which lies in  $\partial\mathcal{H}^2$ , i.e. that  $|\text{tr}(\gamma)| = 2$ .

Every cusp group  $\Delta_\Gamma(p)$  is conjugate in  $\text{PSL}_2(K)$  to  $\Delta_\Gamma(\infty, \infty)$  [17, §5.1]. Thus we take  $p = (\infty, \infty)$ , abbreviate  $\Delta := \Delta_\Gamma(p)$  and  $U := U_\Gamma(p)$ , and this incurs no loss of generality in discussing the cusp shape. We denote  $(\mathcal{H}^2 \times \mathcal{H}^2)/\Delta$  by  $M_\Delta$  and observe that in a small neighborhood of the cusp,  $M_\Gamma$  and  $M_\Delta$  coincide. Such a neighborhood is called a *cusp end*, defined up to homeomorphism.

Matrices in  $\Delta$  are upper triangular, forcing their diagonal entries to be in the unit group  $\mathbb{Z}_K^\times$ . But since  $K$  is a real quadratic field,  $\mathbb{Z}_K^\times = \{\pm\varepsilon^\ell \mid \ell \in \mathbb{Z}\}$  where  $\varepsilon$  is the *fundamental unit* of  $\mathbb{Z}_K$ , defined by  $\varepsilon := \min\{z \in \mathbb{Z}_K^\times \mid z > 1\}$  (see [1] for additional characterizations). Thus we have

$$\Delta = \left\{ \begin{pmatrix} \varepsilon^\ell & z \\ 0 & \varepsilon^{-\ell} \end{pmatrix} \mid \ell \in \mathbb{Z}, z \in \mathbb{Z}_K \right\}$$

up to  $\pm 1$ , recalling that opposite signs are identified in  $\text{PSL}_2(\mathbb{R})$ .

Let  $\tau_z := \begin{pmatrix} 1 & z \\ 0 & 1 \end{pmatrix}$  where  $z \in \mathbb{Z}_K$ . Then  $\forall z \in \mathbb{Z}_K$ ,

$$(1) \quad \tau_z(x_1 + y_1i, x_2 + y_2i) = ((x_1 + z) + y_1i, (x_2 + \sigma(z)) + y_2i),$$

affecting only the real parts of the points. A computation using the trace shows that  $U = \{\tau_z \mid z \in \mathbb{Z}_K\}$ , hence  $U = \langle \tau_1, \tau_\alpha \rangle$ .

Let  $\eta_\ell := \begin{pmatrix} \varepsilon^\ell & 0 \\ 0 & \varepsilon^{-\ell} \end{pmatrix}$ , then

$$(2) \quad \eta_\ell(x_1 + y_1i, x_2 + y_2i) = (\varepsilon^{2\ell}(x_1 + y_1i), \varepsilon^{-2\ell}(x_2 + y_2i)).$$

Let  $D := \{\eta_\ell \mid \ell \in \mathbb{Z}\}$ , then  $D = \langle \eta_1 \rangle$  and  $\Delta = \langle \tau_1, \tau_\alpha, \eta_1 \rangle$ . The full Hilbert-Blumenthal group is attained by including, in the generators, the element  $\iota := \begin{pmatrix} 0 & 1 \\ -1 & 0 \end{pmatrix}$ , an inversion through the unit hemisphere in each factor. That is  $\Gamma = \langle \tau_1, \tau_\alpha, \eta_1, \iota \rangle$ .

The cusp group  $\Delta$  admits a semidirect product decomposition, as follows. The group  $U$  is a normal subgroup of  $\Delta$  and since  $\mathbb{Z}_K \cong \mathbb{Z} \oplus \mathbb{Z}\alpha$  as an additive group,  $U \cong \mathbb{Z}^2$ . Also,  $D \cong \mathbb{Z}$  is a cyclic subgroup of  $\Delta$  and  $U$  is invariant under conjugation by  $D$ , in particular

$\eta_\ell \cdot \tau_z \cdot \eta_{-\ell} = \tau_{2\ell z}$ . This action by conjugation defines a homomorphism  $D \rightarrow \text{Aut}(U)$ , giving

$$(3) \quad \Delta \xrightarrow{\cong} U \rtimes D : \quad \begin{pmatrix} \varepsilon^\ell & z \\ 0 & \varepsilon^{-\ell} \end{pmatrix} \mapsto (\tau_z, \eta_\ell).$$

This admits the topological interpretation that  $M_\Delta$  is diffeomorphic to  $T_\varphi^3 \times \mathbb{R}^+$ , where  $T_\varphi^3$  is the infrasolv manifold (in the sense of [17, §2.4.3]) that fibers over the circle, with fiber the torus, and Anosov diffeomorphism  $\varphi$  [18]. We call  $T_\varphi^3$  the *cuspidal section* of  $M_\Gamma$  (or equivalently, of  $\Gamma$ ).

**2.2. Fundamental domains.** A *fundamental domain* for a group  $G$  acting on a topological space  $\mathcal{X}$  is a subspace of  $\mathcal{X}$ , which we denote by  $R_G(\mathcal{X})$  (or just  $R_G$  when  $\mathcal{X}$  is clear) such that  $\bigcup_{g \in G} g(R_G) = \mathcal{X}$ , and for all pairs  $g, g' \in G$ , the intersection  $g(R_G) \cap g'(R_G)$  has no interior. Notice that this notation does not indicate any specific choice for the domain, and we will introduce different notation when we wish to indicate our particular construction.

Some aspects of fundamental domains  $R_\Gamma(\mathcal{H}^2 \times \mathcal{H}^2)$  have remained consistent since the classical approach while others have varied. A common theme is the use of an intersection of some choices for  $R_U$ ,  $R_D$ , and  $R_{\langle \iota \rangle}$ , to attain an initial approximation of the domain, formalized by Götzky [12] and later termed a Götzky region [10]. Usually, this properly contains a fundamental domain for  $\Gamma$ , and the boundary intersecting  $R_{\langle \iota \rangle}$  is difficult to describe (see Remark 2.3). However,  $R_U \cap R_D$  forms a true fundamental domain for the group  $\Delta$  due to the semidirect product structure  $\Delta \cong U \rtimes D$ .

**2.2.1.  $R_D$  and  $\mathcal{R}_D$ .** This aspect has remained consistent in the literature since Blumenthal [3], and will be used here as well up to a minor alteration. For each  $y_1, y_2 \in \mathbb{R}^+$ , let

$$(4) \quad \mathcal{F}(y_1, y_2) := \{(x_1 + y_1 i, x_2 + y_2 i) \mid x_1, x_2 \in \mathbb{R}\} \subset \mathcal{H}^2 \times \mathcal{H}^2,$$

the pair of horizontal lines at  $y_1$  in the first factor and at  $y_2$  in the second factor. Observe that

$$\bigsqcup_{y_1, y_2 \in \mathbb{R}^+} \mathcal{F}(y_1, y_2) = \mathcal{H}^2 \times \mathcal{H}^2,$$

so  $\mathcal{F} := \{\mathcal{F}(y_1, y_2) \mid y_1, y_2 \in \mathbb{R}^+\}$  foliates  $\mathcal{H}^2 \times \mathcal{H}^2$ . There is a natural bijection

$$(5) \quad \Pi : \mathcal{F} \rightarrow \mathbb{R}^+ \times \mathbb{R}^+, \quad \mathcal{F}(y_1, y_2) \mapsto (y_1, y_2).$$

By (2),  $D$  permutes the leaves via

$$(6) \quad \eta_\ell(\mathcal{F}(y_1, y_2)) = \mathcal{F}(\varepsilon^{2\ell} y_1, \varepsilon^{-2\ell} y_2),$$

thus in the image under  $\Pi$ ,  $D$  preserves each hyperbola in the set  $\{y_1 y_2 = c \mid y_1, y_2 \in \mathbb{R}^+\}_{c \in \mathbb{R}^+}$ , which foliates  $\mathbb{R}^+ \times \mathbb{R}^+$  under  $\Pi^{-1}$ .

A natural fundamental domain for the action of  $D$  is thus obtained as the image under  $\Pi^{-1}$  of the wedge between a pair of rays approaching the origin, identified by  $\eta_1$ . We differ

from the classical approach in how we choose the pair of rays, (justified in §4), and define our fundamental domain for  $D$  as

$$(7) \quad \mathcal{R}_D := \Pi^{-1} \left( \{(y_1, y_2) \in \mathbb{R}^+ \times \mathbb{R}^+ \mid y_2 \leq y_1 < \varepsilon^4 y_2\} \right).$$

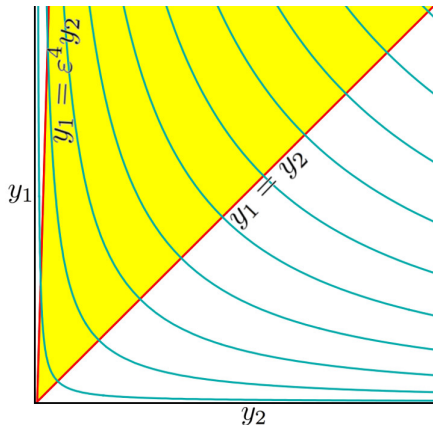


FIGURE 1. [14] The fundamental domain  $\mathcal{R}_D$  is shown (in yellow), for the action of  $D$  on  $\mathcal{F}$ , along with a  $D$ -invariant foliation by hyperbolas (in cyan).

2.2.2.  **$R_U$ .** By (1),  $U$  fixes each leaf of the foliation  $\mathcal{F}$ , and since  $\Delta = U \rtimes D$ , we have that  $R_U \cap \mathcal{R}_D$  is a fundamental domain for  $\Delta$  regardless of one's choice of  $R_U$ . Topologically, each quotient  $\mathcal{F}(y_1, y_2)/U$  is a flat torus and  $\mathcal{F}/U$  is foliated by these tori. If one is interested in arithmetic properties of  $M_\Gamma$  as a topological manifold, one can represent orbits of  $U$  as Siegel [19] does, using a reduction with respect to the field norm on  $K$ , but we are interested in a more geometrically accurate description which, in the following ways, resembles the classical approach.

Define the *height* of a leaf  $\mathcal{F}(y_1, y_2)$  in the foliation  $\mathcal{F}$ , or of a point  $(x_1 + y_1i, x_2 + y_2i)$  in the leaf, as the product  $y_1 y_2$ . A set of points at some fixed height corresponds to the image under  $\Pi^{-1}$  of a hyperbola in Figure 1. Also, under  $\Pi^{-1}$ , a set of tori at the piece of a hyperbola between the rays  $y_1 = y_2$  and  $y_1 = \varepsilon^4 y_2$  gives a geometric representation of the cusp section  $T_\varphi^3$ , and the tori at the entire wedge between these rays gives a diffeomorphic representation of the cusp end.

Define the *level* of a ray as in Figure 1, or of a point  $(x_1 + y_1i, x_2 + y_2i)$  in a leaf on this ray, as the quotient  $y_1/y_2$ . There is a natural bijection at each leaf

$$(8) \quad \pi_{y_1, y_2} : \mathcal{F}(y_1, y_2) \rightarrow \mathbb{R}^2, \quad (x_1 + y_1i, x_2 + y_2i) \mapsto (x_1, x_2).$$

Under these bijections, points at the same level (varying the height) correspond to spaces where the metric scales uniformly, and points at the same height (varying the level) correspond to spaces where the metric expands along one axis and contracts along another.

The classical approach to  $R_U$  is to use the same rectangle for every torus in the foliation, making  $R_U$  an infinitely tall parallelepiped. While this gives a straightforward fundamental

domain for  $\Delta$  in analogy to the classical cusp group of  $\mathrm{PSL}_2(\mathbb{Z})$ , it does not account for the change in metric that occurs in the leaves as the level varies, and obscures the action of  $\varphi$  as a side-pairing upon passing to the quotient  $\mathbb{T}_\varphi^3$ . We will represent (in §3) the orbit of  $U$  by tori that change shape with the deforming metric as the leaves vary, allowing us to write  $\varphi$  explicitly.

**Remark 2.3.** *The classical choice for  $R_{\langle U \rangle}$  is  $\{p \in \mathcal{H}^2 \times \mathcal{H}^2 \mid |p_1| |p_2| \geq 1\}$ . Cohn [7, 6, 8, 9] studied how to approximate a fundamental domain for all of  $\Gamma$  by intersecting this with the classical parallelepiped model of  $R_U$ . He found that in all but the case  $K = \mathbb{Q}(\sqrt{5})$ , this has an infinite-volume boundary due to 3-dimensional regions approaching  $\partial(\mathcal{H}^2 \times \mathcal{H}^2)$ . He introduced the notion of the “floor” as an alternative representation of this boundary, having finite volume at the sacrifice of connectedness. The current authors explored applications to this of our new choice for  $R_U$ , but found the slight improvements not worth the computational complexity.*

**2.2.3. Dirichlet domains.** When  $\mathcal{X}$  is a metric space, we can use its metric to form a type of fundamental domain with additional geometric properties.

**Definition 2.4.** *Let  $G$  be a group of isometries acting on a topological space  $\mathcal{X}$ , let  $d_{\mathcal{X}}$  be a metric on  $\mathcal{X}$ , and let  $c \in \mathcal{X}$  satisfy  $\Delta_G(c) = \{1\}$ . Then the Dirichlet domain for  $G$  with respect to  $d_{\mathcal{X}}$ , centered at  $c$ , is*

$$\mathcal{D}_c(G) := \left\{ x \in \mathcal{X} \mid \forall \gamma \in \Gamma, d_{\mathcal{X}}(c, x) \leq d_{\mathcal{X}}(c, \gamma(x)) \right\}.$$

Then  $\mathcal{D}_c(G)$  is convex and tiles  $\mathcal{X}$  under the group action. Each pair of sides of  $\mathcal{D}_c(G)$  is contributed by an isometry and its inverse, which are identified by that isometry under the group action. The set of isometries that contribute the sides of  $\mathcal{D}_c(G)$  generate the group  $G$ , and when  $G$  is finitely generated, so will be the number of sides. [11]

We can identify  $\mathcal{D}_c(G)$  and its sides with the following tools.

**Definition 2.5.** *Let  $\mathcal{X}$ ,  $G$  and  $c$  be as in Definition 2.4. Let  $p, q \in \mathcal{X}$  with  $p \neq q$ . The semispace contributed (to  $\mathcal{D}_c(G)$ ) by  $g$  (with respect to  $d_{\mathcal{X}}$ ) is*

$$E_c(g) := \{x \in \mathcal{X} \mid d_{\mathcal{X}}(x, c) \leq d_{\mathcal{X}}(g(x), c)\},$$

and the mediatrize contributed (to  $\mathcal{D}_c(G)$ ) by  $g$  (with respect to  $d_{\mathcal{X}}$ ) is the set of points at equality.

Thus,

$$\mathcal{D}_c(G) = \bigcap_{g \in G \setminus \{1\}} E_c(g)$$

and, since  $m_c(g) = \partial E_c(g)$ , each side of  $\mathcal{D}_c(G)$  is a portion of a mediatrize. A convenient characterization of  $m_c(g)$  is as the set of points equidistant from  $c$  and  $g^{-1}(c)$ . To see this, take the defining equation for  $m_c(g)$  and apply the isometry  $g^{-1}$  to the arguments of the distance function on the right hand side. That is,

$$(9) \quad m_c(g) = \{x \in \mathcal{X} \mid d_{\mathcal{X}}(x, c) = d_{\mathcal{X}}(x, g^{-1}(c))\}.$$

**Remark 2.6.** *We prefer the Spanish term “mediatriz” (plural: “mediatrices”) to the more common term “perpendicular bisector,” usually defined with respect to the geodesic from  $c$  to  $g^{-1}(c)$ . Our reason is that a pair of distinct points in  $\mathcal{H}^2 \times \mathcal{H}^2$  does not have a unique geodesic connecting them, since its metric is the  $\ell^1$  sum over the  $\mathcal{H}^2$  metrics, similarly to how the Manhattan metric does not give unique geodesics.*

Our main result, Theorem 4.3, is phrased in terms of notation constructed throughout the article, in such a way that the proof is provided by the content up to the statement of the theorem. The idea is to create a geometrically accurate fundamental domain for  $\Delta$ , and give an algorithm to find the sides of each cusp section  $T_\varphi^3$  along with their gluing maps, including the Anosov diffeomorphism.

### 3. LATTICE DEFORMATIONS

In this section, we construct a fundamental domain for  $U$  as a union of Dirichlet domains for its action on the leaves of the foliation  $\mathcal{F}$ . Consider the function

$$(10) \quad \delta : (\mathcal{H}^2 \times \mathcal{H}^2) \times (\mathcal{H}^2 \times \mathcal{H}^2) \rightarrow \mathbb{R}^{\geq 0},$$

$$((p_1, p_2), (q_1, q_2)) \mapsto \frac{|p_1 - q_1|^2}{\Im(p_1)\Im(q_1)} + \frac{|p_2 - q_2|^2}{\Im(p_2)\Im(q_2)}.$$

We will use  $\delta$  to describe the sides of our fundamental domain as solution sets to cubic polynomials.

**Remark 3.1.** *By way of motivation,  $\delta$  is a simplification of the standard metric on  $\mathcal{H}^2 \times \mathcal{H}^2$  formed by eliminating reliance on transcendental functions. This grants us more manageable computations at the sacrifice of the triangle inequality. That is,  $\delta$  is not a metric on  $\mathcal{H}^2 \times \mathcal{H}^2$ , but a semi-metric. Lemma 3.2 sets us up to use  $\delta$  as desired regardless, and its proof illustrates the specific relationship between  $\delta$  and the standard metric.*

For each  $y_1, y_2 \in \mathbb{R}^+$ , let

$$\delta_{y_1, y_2} := \delta|_{\mathcal{F}(y_1, y_2) \times \mathcal{F}(y_1, y_2)}.$$

For part (3) below, recall from §2.1 the notation  $\tau_z = \begin{pmatrix} 1 & z \\ 0 & 1 \end{pmatrix}$  where  $z \in \mathbb{Z}_K$ , and that elements of this form comprise the group  $U$ . Also, we abbreviate  $E_{(y_1 i, y_2 i)}$  by  $E_{y_1, y_2}$ , and  $m_{(y_1 i, y_2 i)}$  by  $m_{y_1, y_2}$ , and these always denote subsets of the leaf  $\mathcal{F}(y_1, y_2)$ .

**Lemma 3.2.**

- (1) *The function  $\delta$  is invariant under the action of  $\mathrm{PSL}_2(\mathbb{R})$ .*
- (2) *For each  $y_1, y_2 \in \mathbb{R}^+$ , the restriction  $\delta_{y_1, y_2}$  is a metric on the leaf  $\mathcal{F}(y_1, y_2)$ .*
- (3) *Within the leaf  $\mathcal{F}(y_1, y_2)$  and with respect to the metric  $\delta_{y_1, y_2}$ , the semispace  $E_{y_1, y_2}(\tau_z)$  is the solution set to*

$$\frac{2x_1 z + z^2}{y_1^2} + \frac{2x_2 \sigma(z) + \sigma(z)^2}{y_2^2} \geq 0$$

*and the mediatriz  $m_{y_1, y_2}(\tau_z)$  is the set of points at equality.*

*Proof.* The standard distance formula on  $\mathcal{H}^2$  is

$$d_{\mathcal{H}^2}(w, z) = \log \left( x + \sqrt{x^2 - 1} \right)$$

where

$$x = 1 + \frac{|z - w|^2}{2\Im w \Im z},$$

so all dependence of  $d_{\mathcal{H}^2}(w, z)$  on  $w$  and  $z$  occurs in the term  $\frac{|z - w|^2}{\Im w \Im z}$ . Since  $d_{\mathcal{H}^2}$  is invariant under the action of  $\mathrm{PSL}_2(\mathbb{R})$ , so is this term, and since  $\delta$  the sum over such terms,  $\delta$  inherits that property as well.

To prove part (2), recall the definition of  $\mathcal{F}(y_1, y_2)$  from (4), and let  $p, q \in \mathcal{F}(y_1, y_2)$ . Then  $\exists x_1, x_2, x_3, x_4 \in \mathbb{R}$  such that  $p = (x_1 + iy_1, x_2 + iy_2)$  and  $q = (x_3 + iy_1, x_4 + iy_2)$ , and, using (10), we compute

$$(11) \quad \delta_{y_1, y_2}(p, q) = y_1^{-2}|x_1 - x_3|^2 + y_2^{-2}|x_2 - x_4|^2.$$

Each summand is a metric on  $\mathbb{R}$ , obtained by scaling the squared Euclidean metric by a positive constant. The result follows because the sum is the  $\ell^1$  metric over these on  $\mathbb{R}^2 = \pi_{y_1, y_2}(\mathcal{F}(y_1, y_2))$ .

For part (3), recalling Definition 2.4,  $E_{y_1, y_2}(\tau_z)$  is the solution set in  $\mathcal{F}(y_1, y_2)$  to the inequality

$$\delta_{y_1, y_2}((x_1 + y_1 i, x_2 + y_2 i), (y_1 i, y_2 i)) \leq \delta_{y_1, y_2}(\tau_z(x_1 + y_1 i, x_2 + y_2 i), (y_1 i, y_2 i)),$$

and  $m_{y_1, y_2}(\tau_z)$  is the set of points at equality. Carrying out the action of  $\tau_z$ , the right hand side of this is  $\delta(x_1 + z + y_1 i, x_2 + \sigma(z) + y_2 i), (y_1 i, y_2 i)$  where  $\sigma$  is the non-trivial element of the Galois group  $\mathfrak{S}(K : \mathbb{Q})$  (and observe that  $x_1 + z, x_2 + \sigma(z) \in \mathbb{R}$ ). Next, rewrite each side of the inequality according to (11). Rearranging terms (notice that the  $x_1^2$  and  $x_2^2$  terms cancel) yields the desired formula.  $\square$

For each pair  $y_1, y_2 \in \mathbb{R}^+$ , let  $T(y_1, y_2) := \mathcal{D}_{(y_1 i, y_2 i)}(U)$ , the Dirichlet domain for the action of  $U$  on the leaf  $\mathcal{F}(y_1, y_2)$  with respect to the metric  $\delta_{y_1, y_2}$ , centered at  $(y_1 i, y_2 i)$ . As discussed in 2.2.2, these  $T(y_1, y_2)$  slices are flat tori which, ranging over  $y_1, y_2 \in \mathbb{R}^+$ , foliate  $(\mathcal{H}^2 \times \mathcal{H}^2)/U$ . We choose our fundamental domain for  $U$  to be the union of these slices,

$$(12) \quad \mathcal{R}_U := \bigsqcup_{y_1, y_2 \in \mathbb{R}} T(y_1, y_2).$$

Similarly, we extend the semispaces and mediatrices from the leaves across  $\mathcal{H}^2 \times \mathcal{H}^2$ , and introduce the following notation. For  $z \in \mathbb{Z}_K$ , define

$$E(z) := \bigsqcup_{y_1, y_2 \in \mathbb{R}} E_{y_1, y_2}(\tau_z), \text{ and}$$

$$m(z) := \bigsqcup_{y_1, y_2 \in \mathbb{R}} m_{y_1, y_2}(\tau_z),$$



so that  $E(z) \cap \mathcal{F}(y_1, y_2) = E_{y_1, y_2}(\tau_z)$  and  $m(z) \cap \mathcal{F}(y_1, y_2) = m_{y_1, y_2}(\tau_z)$ . Then some collection of the  $m(z)$  (over  $z \in \mathbb{Z}_K \setminus \{0\}$ ) form the sides of  $\mathcal{B}_U$ , and (from Lemma 10, part (3)) each  $m(z)$  is an algebraic variety in  $\mathcal{H}^2 \times \mathcal{H}^2$  defined by the cubic polynomial

$$(13) \quad 2zx_1 + z^2 + \left(\frac{y_1}{y_2}\right)^2 (2\sigma(z)x_2 + \sigma(z)^2) = 0$$

in the four variables  $x_1, x_2 \in \mathbb{R}$ , and  $y_1, y_2 \in \mathbb{R}^+$ .

The next lemma evokes the projections  $\pi_{y_1, y_2} : \mathcal{F}(y_1, y_2) \rightarrow \mathbb{R}^2$  defined by (8). We have  $\pi_{y_1, y_1}(c) = (0, 0)$ , and the orbit of  $(0, 0)$  under  $U$  in this projection is the same for all  $y_1, y_2$ , yet  $\pi_{y_1, y_2}(m_{y_1, y_2}(z))$  depends on  $y_1$  and  $y_2$  due to the scaling from one local metric to another.

**Lemma 3.3.**

- (1) *The projection  $\pi_{y_1, y_2}(m_{y_1, y_2}(\tau_z)) \subset \mathbb{R}^2$  is a Euclidean line.*
- (2) *The pair of lines  $\pi_{y_1, y_2}(m_{y_1, y_2}(\tau_z))$  and  $\pi_{y_1, y_2}(m_{y_1, y_2}(\tau'_z))$  are parallel if and only if  $\exists q \in \mathbb{Q}$  such that  $z' = qz$ .*
- (3) *If  $\frac{y_1}{y_2} = \frac{y'_1}{y'_2}$ , then  $\pi_{y_1, y_2}(T(y_1, y_2)) = \pi_{y'_1, y'_2}(T(y'_1, y'_2))$ .*
- (4) *For each  $y_1, y_2 \in \mathbb{R}^+$ ,  $\pi_{y_1, y_2}(T(y_1, y_2))$  is symmetric about  $(0, 0)$ , is either a parallelogram or a hexagon, and these deform continuously with  $y_1, y_2$ .*

*Proof.* By Lemma 3.2 (3), the mediatriz  $m_{y_1, y_2}(\tau_z) \subset \mathcal{F}(y_1, y_2)$  is the solution set to equation (13) in the  $(x_1, x_2)$ -coordinates, and  $T(y_1, y_2)$  is bounded by these mediatrices. Parts (1) and (3) follow immediately. Part (2) follows from the fact that  $\forall z \in \mathbb{Z}_K$  and  $\forall q \in \mathbb{Q}$ ,  $\sigma(qz) = q\sigma(z)$ .

Since  $\{(z, \sigma(z)) \mid z \in \mathbb{Z}_K\} \subset \mathbb{R}^2$  is discrete, there are finitely many lines  $\pi_{y_1, y_2}(m_{y_1, y_2}(\tau_z))$  contributing sides to  $\pi_{y_1, y_2}(T(y_1, y_2))$ . Altering the level  $y_1/y_2$  in (13) deforms these lines continuously and, since  $\sigma(-z) = -\sigma(z)$ , they occur in pairs  $\pi_{y_1, y_2}(m_{y_1, y_2}(\pm z))$  arranged symmetrically about the origin. Since  $T(y_1, y_2)$  is a Dirichlet domain for the action of  $U$  on  $\mathcal{F}(y_1, y_2)$ , we know that  $\pi_{y_1, y_2}(T(y_1, y_2))$  is convex and tiles the plane via translational symmetry. The only possible number of sides for a convex Euclidean polygon that does this are 3, 4 and 6, but since  $T(y_1, y_2)$  has order 2 rotational symmetry, the number of sides must be 4 or 6.  $\square$

Lemma 3.3 tells us that along each fixed height  $y_1 y_2$  (a 3-dimensional space along a hyperbola in Figure 1; see §2.2.2), the fundamental domain  $\mathcal{B}_U$  has the same 3-dimensional shape: a continuum of parallelograms and hexagons arranged symmetrically about a central axis. We next gain an explicit description of this by controlling the distribution of the parallelograms, as well as which  $z \in \mathbb{Z}_K$  contribute them.

**Proposition 3.4.** *In the 3-dimensional subspace of  $\mathcal{B}_U$  at some fixed height, the parallelogram cross-sections are distributed discretely along the axis of symmetry in the following way. If  $T(y_1, y_2)$  is a parallelogram whose sides are contributed by  $\pm z, \pm z' \in \mathbb{Z}_K$  (choosing*

$z, z' > 0$ ), then  $y_1/y_2 = \sqrt{\frac{-zz'}{\sigma(zz')}}$ . The next parallelogram as  $y_1/y_2$  increases is contributed by  $\pm(z+z')$  and whichever of the pairs  $\pm z$  or  $\pm z'$  that has smaller absolute value under  $\sigma$ .

*Proof.* Recall (from §2.2.2), the level of a point  $(x_1 + iy_1, x_2 + iy_2)$  is  $y_1/y_2$ , and we'll now denote this by  $k$ . By Lemma 3.3 (3), it suffices to look at  $T(k, 1)$ . For  $z \in \mathbb{Z}_K$ , denote the line  $\pi_{k,1}(m_{k,1}(z)) \subset \mathbb{R}^2$  by  $l_z$ . Now fix  $z, z' \in \mathbb{Z}_K^+$  so that  $l_{\pm z}$  and  $l_{\pm z'}$  bound a parallelogram cross section at a fixed height of  $\mathcal{R}_U$ , and denote this parallelogram by  $P$ . Using (13) to write the equations for  $l_z, l_{z'}$ , and  $l_{z+z'}$ , we compute that these have a common intersection point if and only if  $k = \sqrt{\frac{-zz'}{\sigma(zz')}}$ . Thus  $l_{-(z+z')}$  passes through the opposite corner of  $P$  and, by a similar computation, the lines  $l_{\pm(z-z')}$  pass through the other pair of opposite corners of  $P$ . By hypothesis, no lines contributed by  $\mathbb{Z}_K$  enter  $P$  and observe also that no others pass through its corners: indeed  $z$  and  $z'$  are independent, so that any other element of  $\mathbb{Z}_K$  could be written as  $az + bz'$  (with  $a, b \in \mathbb{Z}$  not both  $\pm 1$ ), and a similar computation shows that  $l_{az+bz'}$  cannot pass through these corners at this height.

Now, increasing  $k$  slightly changes the slopes of the lines so that  $l_{z+z'}$  enters the (stretching) parallelogram bounded by  $l_{\pm z}$  and  $l_{\pm z'}$ , and  $l_{z-z'}$  moves away from it. Decreasing  $k$  slightly has the opposite effect. (Figure 2 shows an example of this.) Since this forms

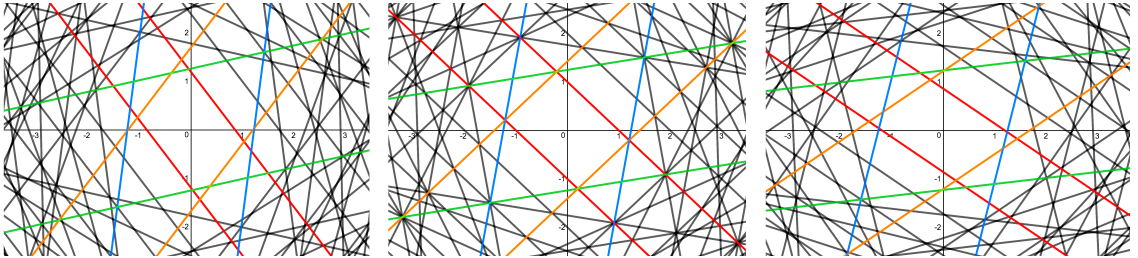


FIGURE 2. [5] Some mediatrices  $\{m(\tau_z) \cap \mathcal{F}(k, 1) \mid z \in \mathbb{Z}_K\}$  in the case  $n = 2$  exemplify the situation described in the proof of Proposition 3.4. The mediatrices at height  $y_1/y_2 = 1$  are in the center, and those with  $y_1/y_2$  slightly decreased and increased are shown on the left and right, respectively. The pairs of mediatrices for  $z = \pm 1, \pm\sqrt{n}, \pm(1 + \sqrt{n})$  and  $\pm(1 - \sqrt{n})$  are colored red, orange, blue, and green, respectively, and the mediatrices for all other  $z \in \mathbb{Z}_K$  that enter the shown region are shown in black. Note that when  $n \equiv_4 1$ , this will occur at heights other than 1.

a hexagon, Lemma 3.3 tells us that no other elements of  $\mathbb{Z}_K$  can simultaneously truncate more corners. Thus  $P$  is a parallelogram precisely at  $k = \sqrt{\frac{-zz'}{\sigma(zz')}}$  and, as the level increases,  $l_{\pm(z+z')}$  contributes a new pair of sides that persist until the next parallelogram is formed. These parallelograms are discretely distributed due to the discreteness of  $\{(z, \sigma(z)) \mid z \in \mathbb{Z}_K\}$ .

Lastly, again analyzing the slopes of the lines as the level  $k$  increases, we see that  $l_{\pm z}$  move outside of  $P$  if and only if  $|\sigma(z)| < |\sigma(z')|$ , so the one with lower absolute value under  $\sigma$  persists in contributing a boundary as the other ceases to do so.  $\square$

#### 4. THE CUSP SHAPE

Let  $\mathcal{R}_\Delta := \mathcal{R}_U \cap \mathcal{R}_D$ , our choice of fundamental domain for the cusp group  $\Delta$ . We will also sometimes write  $\mathcal{R}_n$  for  $\mathcal{R}_\Delta$  to specify that  $K = \mathbb{Q}(\sqrt{n})$  (and  $\Delta$  is the stabilizer of  $(\infty, \infty)$  in  $\mathrm{PSL}_2(\mathbb{Z}_K)$ ). In this section, we state our main result, Theorem 4.3, deriving a precise description of  $\mathcal{R}_n$  and providing an algorithm for computing it effectively from the fundamental unit  $\varepsilon$  of  $\mathbb{Z}_K$ .

As we saw in the previous section,  $\mathcal{R}_U$  is comprised of equally shaped hypersurfaces, one at each fixed height, which are identical up to uniform scaling of the local metrics. Recall from §2.2.1 that  $\mathcal{R}_D$  is the wedge bounded by the hypersurface at  $y_1 = y_2$  (at level 1) and the hypersurface at  $y_1 = \varepsilon^4 y_2$  (at level  $\varepsilon^4$ ). Let

$$(14) \quad \mathcal{T}_n(h) := \bigsqcup_{1 \leq y < \varepsilon^4} \mathrm{T}(hy, h),$$

and when  $h$  does not matter, we will simply write  $\mathcal{T}_n$ . Then  $\mathcal{T}_n$  is a geometric model for the cusp section and we have  $\mathcal{R}_n = \bigsqcup_{h \in \mathbb{R}^+} \mathcal{T}_n(h)$ .

We will now compute the shapes of the torus slices of  $\overline{\mathcal{T}_n}$  at levels  $(y_1/y_2 =) 1$  and  $\varepsilon^4$ , and see how they glue together under the action of  $D$ . At level 1, we take advantage of the fact that the metric  $\delta_{y_1, y_2}$  is squared Euclidean when  $y_1 = y_2$ . (This was the motivation for our choice of this as a boundary component of  $\mathcal{R}_D$  in §2.2.1.)

#### Lemma 4.1.

(1) If  $n \not\equiv_4 1$ , then  $\pi_{y,y}(\mathrm{T}(y, y))$  is a rectangle whose sides are contributed by

$$\{\tau_z \mid z = \pm 1, \pm\sqrt{n}\}.$$

(2) If  $n \equiv_4 1$ , then  $\pi_{y,y}(\mathrm{T}(y, y))$  is a hexagon whose sides are contributed by

$$\left\{ \tau_z \mid z = \pm 1, \pm \frac{1 + \sqrt{n}}{2}, \pm \frac{1 - \sqrt{n}}{2} \right\}.$$

*Proof.* For an element  $z = a + b\sqrt{n} \in \mathbb{Z}_K$  with  $a, b \in \mathbb{Q}$ , and any  $y_1, y_2 \in \mathbb{R}^+$ , we have

$$(\pi_{y_1, y_2} \circ \tau_z|_{\mathcal{F}(y_1, y_2)})(y_1 i, y_2 i) = (a + b\sqrt{n}, a - b\sqrt{n}).$$

Therefore the orbit of  $U$  on  $(y_1 i, y_2 i)$  at  $\mathcal{F}(y_1, y_2)$  forms a rectangular lattice if  $n \not\equiv_4 1$ , and forms a hexagonal lattice if  $n \equiv_4 1$ , where in both cases the lattice has the diagonal lines of symmetry  $x_1 = \pm x_2$ . Now let  $y_1 = y_2 = y$ . The mediatrices  $m(\tau_z) \cap \mathcal{F}(y, y)$  are the Euclidean perpendicular bisectors between the points  $(0, 0)$  and  $(z, \sigma(z))$ . Thus  $\mathrm{T}(y, y)$  is rectangular if  $n \not\equiv_4 1$  and hexagonal if  $n \equiv_4 1$  (see Figure 3).

In both cases, sides are contributed by the orbit points closest to the origin, which, after projecting by  $\pi_{y,y}$ , are  $\pm(1, 1)$  (contributed by  $\tau_z$  with  $z = \pm 1$ ). Additional sides are then

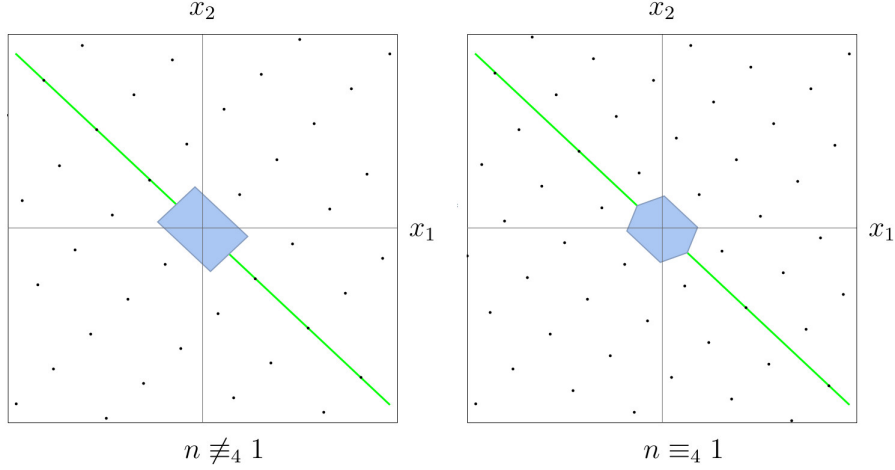


FIGURE 3. [14] The points show the two lattice types formed by the orbit of  $U$  on  $(0, 0)$  under  $\pi_{y_1, y_2}$ , with the line of symmetry  $x_1 = -x_2$  shown in green. The two types of toroidal Euclidean Dirichlet domains when  $y_1 = y_2$  are shown in blue.

contributed by the closest points to the origin that lie between the lines

$$\pi_{y,y}(m_{y,y}(\tau_{\pm 1})) = \{(x_1, x_2) \mid x_1 + x_2 = \pm 1\}.$$

When  $n \not\equiv_4 1$ , these are  $\pm \left(\frac{\sqrt{n}}{2}, -\frac{\sqrt{n}}{2}\right)$  (contributed by  $z = \pm\sqrt{n}$ ) and when  $n \equiv_4 1$ , they are  $\pm \left(\frac{1+\sqrt{n}}{2}, \frac{1-\sqrt{n}}{2}\right)$  and  $\pm \left(\frac{1-\sqrt{n}}{2}, \frac{1+\sqrt{n}}{2}\right)$  (contributed by  $\tau_z$  with  $z = \pm\frac{1+\sqrt{n}}{2}$  and  $\pm\frac{1-\sqrt{n}}{2}$ , respectively).  $\square$

To describe the torus in  $\overline{\mathcal{T}}_n$  at level  $\varepsilon^4$ , and also see how this attaches to the torus at level 1 under the action of  $D$ , we will prove something more general. Recall from (2) that  $\eta_\ell = \begin{pmatrix} \varepsilon^\ell & 0 \\ 0 & \varepsilon^{-\ell} \end{pmatrix}$ , that  $\eta_\ell(x_1 + iy_1, x_2 + iy_2) = (\varepsilon^{2\ell}(x_1 + iy_1), \varepsilon^{-2\ell}(x_2 + iy_2))$ , and that  $\Delta = \langle \eta_1 \rangle$ .

**Lemma 4.2.** *The image under  $\eta_1$  of  $m_{y,y}(\tau_z)$  is  $m_{\varepsilon^2 y, \varepsilon^{-2} y}(\tau_{\varepsilon^2 z})$ .*

*Proof.* The equation defining the mediatriz  $m_{\varepsilon^2 y, \varepsilon^{-2} y}(\tau_{z^2})$  is obtained by taking (13) and substituting  $\varepsilon^2 z$  for  $z$ , and  $\varepsilon^4$  for  $y_1/y_2$ . Recalling that  $\sigma(\varepsilon)^2 = \varepsilon^{-2}$ , this yields

$$2zx_1 + \varepsilon^2 z^2 + 2\varepsilon^4 \sigma(z)x_2 + \varepsilon^2 \sigma(z)^2 = 0.$$

Applying  $\eta_{-1}(= \eta_1^{-1})$  to this line has the effect of sending it to the leaf  $\mathcal{F}(y, y)$  and altering its defining equation by appending a factor of  $\varepsilon^2$  to  $x_1$ , and a factor of  $\varepsilon^{-2}$  to  $x_2$ , after which all the  $\varepsilon$  cancel, leaving the equation for  $m_{y,y}(\tau_z)$ . Thus  $\eta_1^{-1}(m_{\varepsilon^2 y, \varepsilon^{-2} y}(\tau_{\varepsilon^2 z})) = m_{y,y}(\tau_z)$ .  $\square$

Since  $\eta_1$  is an isometry of  $\mathcal{H}^2 \times \mathcal{H}^2$ , Lemma 4.2, implies a one-to-one correspondence between the sides of  $T(\varepsilon^2 y, \varepsilon^{-2} y)$  and the sides of  $T(y, y)$ , as follows:  $\tau_z$  contributes a side to  $T(y, y)$  if and only if  $\tau_{z^2}$  contributes a side to  $T(\varepsilon^2 y, \varepsilon^{-2} y)$ . Moreover,  $\eta_1(T(y, y)) = T(\varepsilon^2 y, \varepsilon^{-2} y)$ , so that  $\eta_1$  is the Anosov diffeomorphism that provides the final side-pairing on  $\mathcal{T}_n$ .

Combining this with the other results thus far completes the geometric description of each fundamental domain  $\mathcal{R}_n$  (over all squarefree  $n \in \mathbb{N}$ ), and gives a straightforward algorithm for computing it. Before we collect these results into our theorem, we provide a map that will make the description more precise and facilitate computations. Let

$$\Psi : \mathcal{H}^2 \times \mathcal{H}^2 \rightarrow \mathbb{R}^3, \quad (x_1 + y_1 i, x_2 + y_2 i) \mapsto (x_1, x_2, \frac{y_1}{y_2}),$$

and write  $k = y_1/y_2$  (the level, as before) for the third coordinate.

**Theorem 4.3.** *For  $K = \mathbb{Q}(\sqrt{n})$  ( $n$  squarefree), a cusp group of the Hilbert-Blumenthal surface  $(\mathcal{H}^2 \times \mathcal{H}^2)/\mathrm{PSL}_2(\mathbb{Z}_K)$  admits a fundamental domain in which each cusp section  $\mathcal{T}_n$  is described as follows.*

### Sides

The region  $\Psi(\mathcal{T}_n)$  lies between the planes at  $k = 1$  and  $k = \varepsilon^4$ . The rest of the sides of  $\Psi(\mathcal{T}_n)$  are the surfaces defined by the cubic polynomials

$$2zx_1 + z^2 + k^2(2\sigma(z)x_2 + \sigma(z)^2) = 0$$

contributed over the  $z \in \mathbb{Z}_K$  that occur in the list  $L$  constructed by the following algorithm.

- (1) Let  $z_1 = 1$ .
  - (a) If  $n \not\equiv_4 1$ , let  $z'_1 = \sqrt{n}$ .
  - (b) If  $n \equiv_4 1$ , let  $z'_1 = \frac{1+\sqrt{n}}{2}$ .
- (2) Let  $z_m = \varepsilon^2 z_1$  and  $z'_m = \varepsilon^2 z'_1$ .
- (3) Start with  $i = 1$ , and while  $\{z_i, z'_i\} \neq \{z_m, z'_m\}$ , let  $z_{i+1} = z_i + z'_i$  and let  $z'_{i+1}$  be the element of  $\{z_i, z'_i\}$  that is minimal under  $|\sigma|$ .
- (4) Let  $L = \{\pm z_1, \pm z'_1, \dots, \pm z_m, \pm z'_m\}$ , and if  $n \equiv_4 1$ , also include  $\sigma(z'_1)$ .

### Torus Shapes

Orthogonal slices of  $\Psi(\mathcal{T}_n)$  along the  $k$ -axis are flat tori. These are all hexagons, with the following exceptions. For  $i < m$ : the sides contributed by  $\pm z_i$  and  $\pm z'_i$  bound a parallelogram at  $k = \sqrt{\frac{-z_i z'_i}{\sigma(z_i z'_i)}}$ . If  $n \not\equiv_4 1$ , this also holds for  $i = m$ , at  $k = \varepsilon^4$  (otherwise, the parallelogram bounded by the surfaces defined by  $\pm z_m$  and  $\pm z'_m$  crosses the  $k$ -axis above  $\Psi(\mathcal{T}_n)$ ).

### Gluing Maps

For each  $\pm z_i$  contributing sides as above, that pair of sides are attached toroidally by  $\tau_{z_i} \in \mathrm{U}$ . Finally, the tori in  $\mathcal{T}_n$  at  $k = 1$  and  $k = \varepsilon^4$  are attached by the Anosov diffeomorphism

$$\eta_1 = \begin{pmatrix} \varepsilon & 0 \\ 0 & \varepsilon^{-1} \end{pmatrix} \in \mathrm{D}. \quad \square$$

**Remark 4.4.** *There will be repetition in the list  $L$ , as  $z'_{i+1}$  is always equal to one of  $z_i$  or  $z'_i$ . This notation agrees with that of Proposition 3.4, where we tracked pairs of isometries by where the parallelogram tori occur.*

**Corollary 4.5.** *Every Sol 3-manifold is commensurable to a manifold admitting the fundamental domain described in Theorem 4.3.*

## 5. EXAMPLES AND VISUALIZATION

We conclude by showing some uses of Theorem 4.3 to study specific examples, focusing on the first two  $n$ -values modulo 4:  $n = 2, 3$  ( $\not\equiv_4 1$ ), and  $n = 5, 13$  ( $\equiv_4 1$ ). Table 1 summarizes three pieces of information that will be important in the calculations. First is the fundamental unit  $\varepsilon$  of each field  $\mathbb{Q}(\sqrt{n})$ , which can be found in (or computed according to) [1]. Second is the sign of the *field norm*

$$N : \mathbb{Z}_K \rightarrow \mathbb{Z}, \quad z \mapsto z \cdot \sigma(z)$$

of each  $\varepsilon$ , noting in particular that this decides the sign in  $\sigma(\varepsilon) = \pm\varepsilon^{-1}$ . We have one of each possible signs in each of our cases for  $n$  modulo 4. Third is an expression showing how to write  $\varepsilon^2$  as a linear combination of 1 and  $\varepsilon$  over  $\mathbb{Z}$ , allowing us to easily reduce the degree of any product of such expressions.

TABLE 1. Some notes to compute our examples

$n$	$\varepsilon$	$N(\varepsilon)$	$\varepsilon^2$
2	$1 + \sqrt{2}$	-1	$1 + 2\varepsilon$
3	$2 + \sqrt{3}$	1	$-1 + 4\varepsilon$
5	$\frac{1+\sqrt{5}}{2}$	1	$1 + \varepsilon$
13	$\frac{3+\sqrt{13}}{2}$	-1	$1 + 3\varepsilon$

Table 2 shows the elements of  $\mathbb{Z}_K$  that contribute sides to  $\mathcal{T}_n$  for  $n = 2, 3, 5$ , and 13. The leftmost column indicates which example is being studied by reminding the reader of the corresponding fundamental unit  $\varepsilon$  (where  $\sqrt{n}$  will appear). The “level” column shows the locations going up the  $k$ -axis where orthogonal slices are parallelograms and, for  $n \equiv_4 1$ , also includes the hexagonal tops and bottoms (otherwise already included). Equivalently, these are the levels along the  $k$ -axis where the edges of the  $\mathcal{T}_n$ , formed by the intersecting sides, bifurcate as a 3-valent graph. The “sides” column lists the elements of  $\mathbb{Z}_K$ , up to sign, that bound the tori at the corresponding levels. The rightmost column shows how those sides correspond to the  $z_i, z'_i$  notation of Theorem 4.3 (and Proposition 3.4), where the indices range over the sequence of parallelograms.

Notice the suggestive occurrence of an additional square root (not in  $K$ ) in the levels when  $N(\varepsilon) = -1$ . For the  $n = 5$  example, we computed a way of expressing these as square roots of  $\varepsilon$ . For the  $n = 13$  example, we see  $\sqrt{3}$  occurring in the denominators.

TABLE 2. levels of  $\mathcal{T}_n$  where edges bifurcate, for  $n = 2, 3, 5,$  and  $13$

$\varepsilon$	level	sides	$i$
$1 + \sqrt{2}$	1	$1, \sqrt{2}$	1
	$\varepsilon$	$1, \varepsilon$	2
	$\varepsilon^2$	$\varepsilon\sqrt{2}, \varepsilon$	3
	$\varepsilon^3$	$\varepsilon^2, \varepsilon$	4
	$\varepsilon^4$	$\varepsilon^2, \varepsilon^2\sqrt{2}$	$5 = m$
$2 + \sqrt{3}$	1	$1, \sqrt{3}$	1
	$\varepsilon^{1/2}$	$1, 1 + \sqrt{3}$	2
	$\varepsilon^{3/2}$	$\varepsilon, 1 + \sqrt{3}$	3
	$\varepsilon^2$	$\varepsilon, \varepsilon\sqrt{3}$	4
	$\varepsilon^{5/2}$	$\varepsilon, \varepsilon(1 + \sqrt{3})$	5
	$\varepsilon^{7/2}$	$\varepsilon^2, \varepsilon(1 + \sqrt{3})$	6
	$\varepsilon^4$	$\varepsilon^2, \varepsilon^2\sqrt{3}$	$7 = m$
$\frac{1 + \sqrt{5}}{2}$	1	$1, \varepsilon, \varepsilon^{-1}$	(hexagonal)
	$\varepsilon$	$1, \varepsilon$	1
	$\varepsilon^3$	$\varepsilon^2, \varepsilon$	$2 = m - 1$
	$\varepsilon^4$	$\varepsilon^3, \varepsilon^2, \varepsilon$	(hexagonal)
$\frac{3 + \sqrt{13}}{2}$	1	$1, \frac{1+\sqrt{13}}{2}, \frac{1-\sqrt{13}}{2}$	(hexagonal)
	$\frac{1+\sqrt{13}}{2\sqrt{3}}$	$1, \frac{1+\sqrt{13}}{2}$	1
	$\varepsilon$	$1, \varepsilon$	2
	$\frac{\varepsilon(1+\varepsilon)}{\sqrt{3}}$	$1 + \varepsilon, \varepsilon$	3
	$\frac{\varepsilon(1+2\varepsilon)}{\sqrt{3}}$	$1 + 2\varepsilon, \varepsilon$	4
	$\varepsilon^3$	$\varepsilon^2, \varepsilon$	5
	$\frac{\varepsilon^2(1+4\varepsilon)}{\sqrt{3}}$	$\varepsilon^2, 1 + 4\varepsilon$	$6 = m - 1$
	$\varepsilon^4$	$\varepsilon^2, 1 + 4\varepsilon, 2 + 7\varepsilon$	(hexagonal)

Figure 4 shows plots of the cusp sections  $\mathcal{T}_n$  for these same examples under the map  $\Psi$ , but with the third coordinate scaled logarithmically in the base  $\varepsilon$ . That is, we are seeing the images of the  $\mathcal{T}_n$  under the map

$$\Psi_n : \mathcal{H}^2 \times \mathcal{H}^2 \rightarrow \mathbb{R}^3, \quad (x_1 + y_1i, x_2 + y_2i) \mapsto (x_1, x_2, \log_\varepsilon (y_1/y_2)).$$

Creating such plots only requires generating a list of the sides, which is a less arduous computation than finding the levels of the parallelograms. Those parallelograms will, of course, occur on their own as a result of how the sides intersect.

The images of  $\Psi_n(\mathcal{T}_n)$  become arbitrarily more complicated and stretched (though not uniformly) as  $n$  increases, making rendering the graphics less feasible for many other cases.

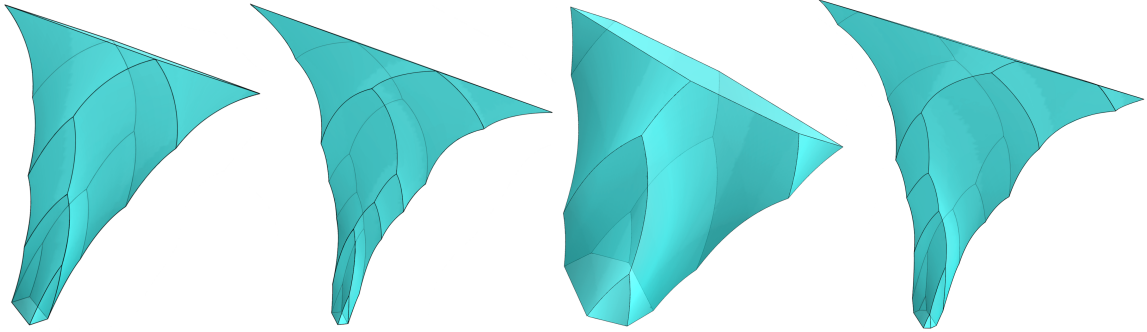


FIGURE 4. [14] Computer generated images are shown of the images of  $\Psi_n(\mathcal{T}_n)$ , for  $n = 2, 3, 5$  and  $13$ , from left to right, respectively.

Another way to study patterns in these shapes, for which computer images are not necessary, is to look at which pairs of sides persist from one parallelogram to the next, going up the  $k$ -axis, and that can be examined via the relatively easy computation of the sides. One interesting approach is to first generate a list like those under the “sides” columns of Table 2, where persisting sides maintain their position among the entries they appear in, and then to draw edges between the different vertical stacks of the same integers. This creates a 3-valent graph that is equivalent (just flipped upside down) to the one seen on the front of the plot of each  $\Psi_n(\mathcal{T}_n)$  in Figure 4, which repeats symmetrically on the back.

This thereby offers some new and fairly accessible techniques by which one might further study quadratic fields, cusp sections of Hilbert-Blumenthal surfaces, and commensurability classes of Sol 3-manifolds.

## 6. ACKNOWLEDGEMENTS

This research paper has been made possible thanks to the financial support generously given by the FORDECyT-CONACyT (Mexico) grant #265667, Universidad Nacional Autónoma de México. The second author was financed by grant IN106817, PAPIIT, DGAPA, Universidad Nacional Autónoma de México. The authors also express their gratitude to Ian Agol, Kathleen Byrne, Jesse Ira Deutsch, Paul Garrett, Ben McReynolds, Jorge Millan and Walter Neumann for helpful suggestions and discussion; to the reviewer for their detailed comments and corrections; and to Dennis Ryan and Simon Woods for help with creating the computer generated images.

## REFERENCES

- [1] Takashi Azuhata. On the fundamental units and the class numbers of real quadratic fields. *Nagoya Mathematical Journal*, 95:125–135, 1984.
- [2] Wolf Barth, Klaus Hulek, Chris Peters, and Antonius Van de Ven. *Compact complex surfaces*, volume 4. Springer, 2015.
- [3] Otto Blumenthal. Über modulfunktionen von mehreren veränderlichen (Erste Hälfte). *Mathematische Annalen*, 56:509–548, 1903.



- [4] Otto Blumenthal. Über modulfunktionen von mehreren veränderlichen (Zweite Hälfte). *Mathematische Annalen*, 58:497–527, 1904.
- [5] Desmos Graphing Calculator. 2017. available at <https://www.desmos.com/calculator>.
- [6] Harvey Cohn. A numerical survey of the floors of various Hilbert fundamental domains. *Mathematics of Computation*, 19(92):594–605, 1965.
- [7] Harvey Cohn. On the shape of the fundamental domain of the Hilbert modular group. In *Proc. Symp. Pure Math*, volume 8, pages 190–202, 1965.
- [8] Harvey Cohn. Note on how Hilbert modular domains become increasingly complicated. *Journal of Mathematical Analysis and Applications*, 15(1):55–59, 1966.
- [9] Harvey Cohn. Some computer-assisted topological models of Hilbert fundamental domains. *Mathematics of Computation*, 23(107):475–487, 1969.
- [10] Jesse Ira Deutsch. Conjectures on the fundamental domain of the Hilbert modular group. *Computers & mathematics with applications*, 59(2):700–705, 2010.
- [11] Peter Engel. Dirichlet domains. In *Geometric Crystallography*, pages 13–21. Springer, 1986.
- [12] Fritz Götzky. Über eine zahlentheoretische anwendung von modulfunktionen zweier veränderlicher. *Mathematische Annalen*, 100(1):411–437, 1928.
- [13] Friedrich Hirzebruch. The Hilbert modular group, resolution of the singularities at the cusps and related problems. In *Séminaire Bourbaki vol. 1970/71 Exposés 382–399*, pages 275–288. Springer, 1971.
- [14] Wolfram Research, Inc. Mathematica, Version 11.1.10. Champaign, IL, 2017.
- [15] Hans Maass. *Über Gruppen von hyperabelschen Transformationen*. Weiss, 1940.
- [16] Curtis T McMullen. Foliations of Hilbert modular surfaces. *American Journal of Mathematics*, pages 183–215, 2007.
- [17] David Ben McReynolds. Cusps of arithmetic orbifolds. *arXiv preprint math/0606571*, 2006.
- [18] David Ben McReynolds. Cusps of Hilbert modular varieties. In *Mathematical Proceedings of the Cambridge Philosophical Society*, volume 144, pages 749–759. Cambridge Univ Press, 2008.
- [19] Carl Ludwig Siegel. On advanced analytic number theory. *Tata Institute for Fundamental Research, Bombay*, 1961.
- [20] Gerard Van Der Geer. *Hilbert modular surfaces*, volume 16. Springer Science & Business Media, 2012.